References and Notes

1. B. C. Murray and M. C. Malin, *Science* **182**, 437 (1973).
2. H. Masursky and N. L. Crabill, *ibid.* **194**, 62 (1976).
3. C. B. Farmer, D. W. Davies, D. D. LaPorte, *ibid.* **193**, 776 (1976).
4. As subsequent events were to prove, the rev 22 observations were invaluable since the polar water vapor began to decrease rapidly thereafter with the onset of lower average temperatures.
5. H. H. Kieffer, S. L. Chase, Jr., E. D. Miner, F. D. Palluconi, G. Munch, G. Neugebauer, T. Z. Martin, *Science* **193**, 780 (1976).
6. H. H. Kieffer, *ibid.* **194**, 1344 (1976).
7. ———, S. L. Chase, Jr., E. Miner, G. Munch, G. Neugebauer, *J. Geophys. Res.* **78**, 4291 (1973).
8. We thank P. Doms, S. Hanson, A. L. Holland, and R. Kares for their assistance with the analysis of the data. This report presents the results of one phase of research carried out at the Jet Propulsion Laboratory under NASA contract NAS 7-100.

18 October 1976

Martian North Pole Summer Temperatures: Dirty Water Ice

Abstract. *Broadband thermal and reflectance observations of the martian north polar region in late summer yield temperatures for the residual polar cap near 205 K with albedos near 43 percent. The residual cap and several outlying smaller deposits are water ice with included dirt; there is no evidence for any permanent carbon dioxide polar cap.*

Observations of the martian south polar cap obtained by Mariner 7 conclusively demonstrated that the seasonal polar caps were composed predominantly of solid CO_2 (*1*). Whether the residual polar caps are composed of H_2O, CO_2, or a combination of them has been the subject of continued debate [for example, see (*2–4*)]. The abundance of martian surface forms attributed to fluvial erosion is a strong indication that Mars previously had a more extensive atmosphere than it does now, and permanent deposits of solid CO_2 have been invoked as stores of material that could contribute to periodic reconstitution of such an atmosphere (*5*). A persistent CO_2 polar cap would also act as a permanent cold trap and strongly influence the transport of water vapor around the planet.

A conclusive test for the absence of solid CO_2 is observation of brightness temperatures appreciably greater than 148 K, the saturation temperature of CO_2 at the martian mean total surface pressure (6.1 mbar). Carbon dioxide can be "condensed" as carbon dioxide–water clathrate ($CO_2 \cdot 6H_2O$), with an effective CO_2 density of about 0.33 g cm^{-3}, at temperatures about 5 K higher than pure CO_2. Considering both the possibility of a clathrate and that the polar surface could be at low elevation (high pressure) (*6*), temperatures above 155 K are incompatible with condensed CO_2 at the martian surface. Conclusive observations were not made by Mariner 9 (*7*).

A major objective of the Viking thermal mapping investigation has been to measure the temperature of the residual north polar cap. The infrared thermal mapper (IRTM) measures the brightness temperature at 18 to 24 μm (T_{20}) and 10 to 13 μm (T_{11}) and the total reflected solar energy (expressed as apparent albedo) simultaneously in seven 5-mrad-diameter spots with three telescopes; the fourth telescope has three detectors each at 7 and 9 μm and one in the 15-μm CO_2 band (*8*).

While the second Viking spacecraft was searching for a suitable landing area, the orbiter infrared instruments made observations which, on several revolutions, extended into the north polar region. On 31 August 1976, coverage of nearly 180° of longitude was obtained with seven accompanying pictures of a portion of the polar cap.

The measurements of 20-μm brightness temperatures over the region of the imaging coverage are shown in Fig. 1. The major thermal boundaries clearly correspond to structure in the visual brightness. The large dark regions have T_{20} near 235 K, while the main portion of

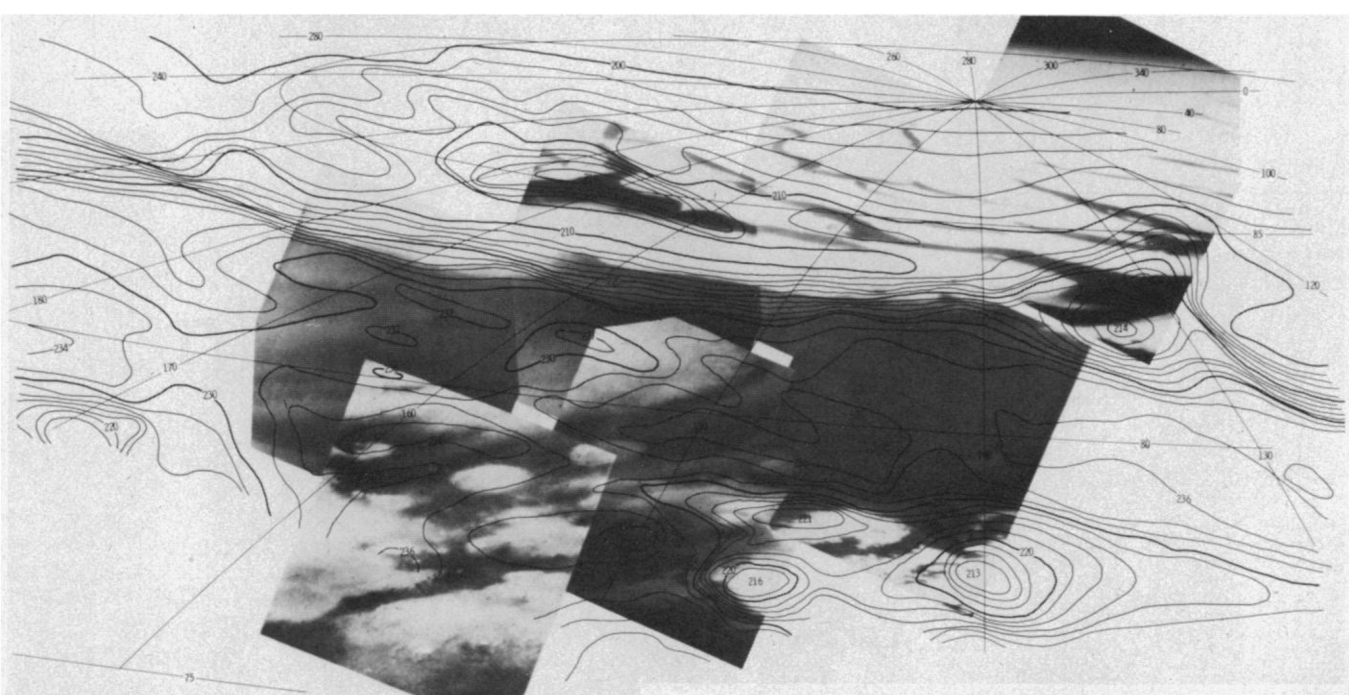

Fig. 1. Contours of T_{20} for part of the 31 August 1976 observations. The circular field of a single IRTM detector has a diameter one-sixth the width of a single photograph. The light areas with temperatures near or below 220 K are water ice. The light areas in the lower left portion of the mosaic are almost entirely clouds with little actual brightness variation; the contrast between adjacent frames indicates the variation of image enhancement. At the center of the mosaic, the geometry at the time of the IRTM observations was: solar incidence angle 62°, viewing angle 70°, phase angle 49°, local time 1500 hours, and range 3200 km.

the residual cap has T_{20} near 205 K. The bright areas near 77°N, 145°W are a frost-filled crater and some adjacent patches which have temperatures of 215 K or less. The warmer region at 84°N, 130°W corresponds to a dark entrant into the cap observed by Mariner 9.

Although there is certainly temperature structure below the resolution of these IRTM observations, the observed temperatures are so high that the presence of CO_2 ice can definitely be excluded. The IRTM bands are sufficiently separated in wavelength that a scene with wide temperature distribution would produce strong apparent spectral dependence. Scenes which were in fact composed of equal areas at 205 K and 240 K would have 3 K difference between T_{20} and T_{11}, approximately that observed in the regions of strong temperature contrasts. At 87°N, 160°W, where the imaging data suggest that there is little dark (warm) material in the IRTM field of view, the brightness temperatures in all bands agree at 205 K within their noise levels. This cannot be accomplished with any mixture of 150 K and 240 K material. Were this scene composed partially of CO_2 ice at 150 K, with the remainder being dark material near 240 K, the fraction of dark material required would have to vary from 29 percent for T_7 to 59 percent for T_{20}. In addition, the albedo of the CO_2 ice would have to exceed unity to fit the observed reflected sunlight. These requirements are independent of the length scale of mixing; in addition, lengths below the order of 1 m are almost certainly incompatible with the necessary temperature differences. The imaging data imply that large (scale larger than 1 km) unfrosted areas comprise at most a few percent of the IRTM field of view at this location.

The T_{11} observations of the north polar region are shown in Fig. 2. The major thermal boundary follows the outline of the bright cap area seen at the end of the Mariner 9 mission, at a season 1½ martian months earlier than the current observations. There are also several local cold areas well separated from the main polar cap. In particular, the 90-km-diameter crater Korolev, at 73°N, 196°W, which was observed near local noon, has T_{11} = 210 K in its interior, while the region immediately surrounding it is near 240 K. In the region of the irregular frost

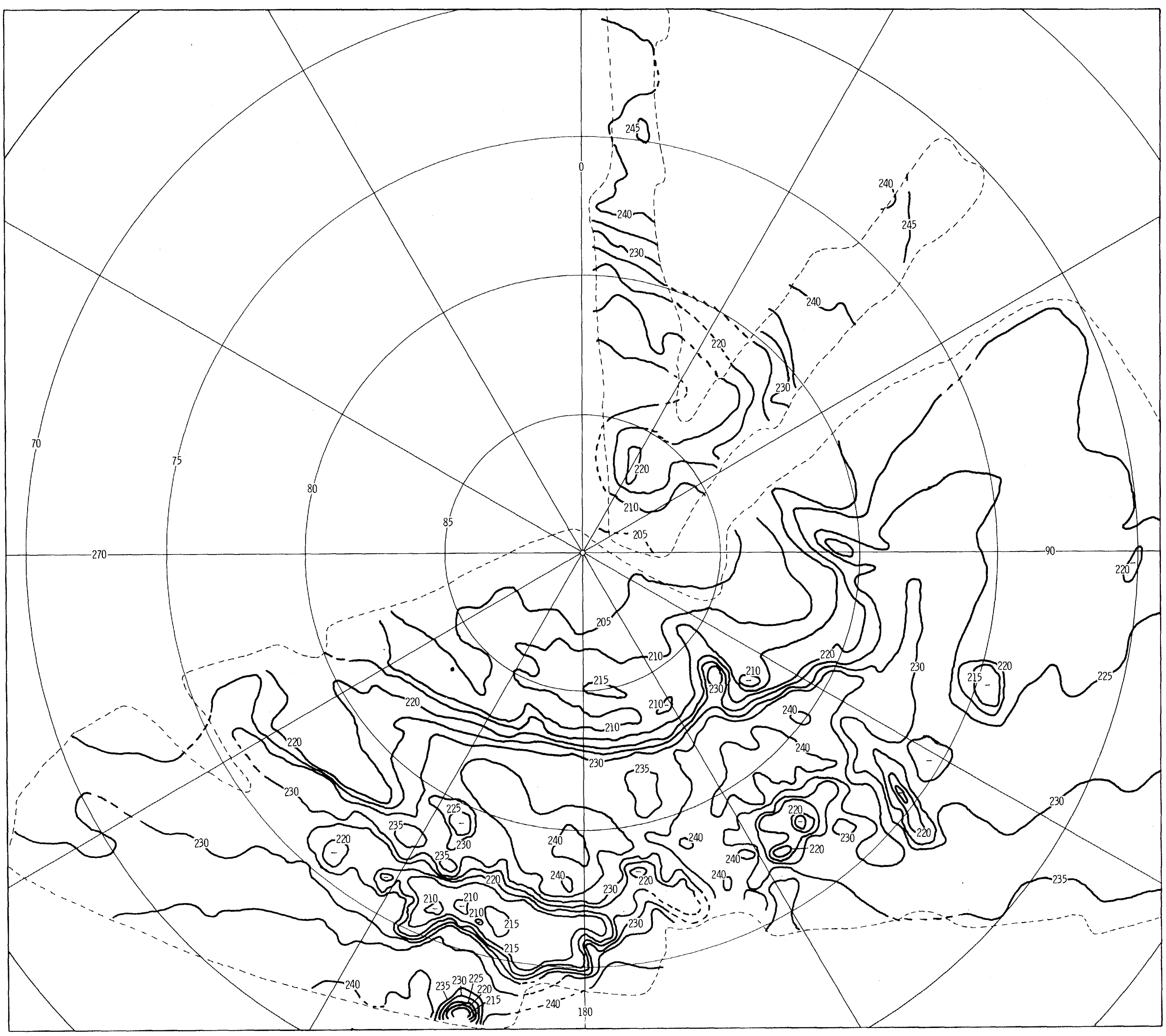

Fig. 2. Polar stereographic projection of T_{11}. The light dashed line indicates the extent of coverage. Closed contours are positive unless identified as negative (−). Near longitude 90°, the apparent decrease of T_{11} at constant latitude is probably due to the very oblique viewing. The center of each of the three sequences was at approximately 1500 hours; no correction for diurnal temperature variation has been made.

patches seen between 75°N, 180°W, and 76°N, 210°W by Mariner 9, T_{11} varies between 209 K and 220 K.

There is a strong correlation between temperature and apparent albedo A measured by the IRTM in the polar region. Nearly all points fall within $T_{20} = 240 - 136\ (A - 0.2) \pm 5$ K, with strong concentrations of data at $A = 0.24 \pm 0.05$ and $A = 0.41 \pm 0.03$; the intermediate points may largely represent observations which include appreciable fractions of both these apparent end members.

There is essentially a one-to-one correlation between areas of high albedo, areas of low temperature, and bright areas seen by Mariner 9 earlier in the summer. All of these areas must be covered with water ice. There is no evidence for any frozen CO_2 in the north polar region at this season (*9*).

The apparent albedo of the polar frosts is much lower than the albedo of clean terrestrial snow deposits (typically greater than 0.7). This could be caused by the frosts having either included dirt or partially glazed surfaces that reflect much of the sunlight in the specular direction, which is not observed by Viking. The simultaneous measurement of thermal emission and reflected solar radiation allows a test of the heat balance to distinguish between these possible explanations.

Assuming that the surface temperature is nearly in equilibrium with the absorbed sunlight, as expected for a water ice deposit, the broadband brightness temperature T and bolometric albedo A_B (the fraction of solar radiation reflected in all directions) will be related by $(T/245)^4 = (1 - A_B)$ at 80°N at this season. This yields $A_B = 0.45$ at 210 K.

This agreement between the inferred bolometric albedo and the apparent albedo implies that the frost does not scatter very anisotropically; therefore, the likely cause of the low albedo is the presence of dirt. This dirt could be brought into the polar regions by the net poleward wind during the fall and winter, by global dust storms, or by both processes.

Several bright areas occur in the southwest portion of the imaging mosaic; although the standard image processing displays some of these areas as nearly as bright as the polar cap, from IRTM measurements the areas have an apparent albedo only 0.02 to 0.05 greater than that of the surface material and a thermal contrast of only about 5 K. They are in several instances associated with ground ice areas, some are nearly circular in horizontal extent, and the largest has periodic cusps along internal bands and near its edge, characteristic of condensate clouds. The small thermal and albedo contrasts across the clouds imply that they are both low and thin; they are almost certainly water ice clouds, indicating that the lower atmosphere is saturated with H_2O.

The T_{15} measurements of the atmosphere covered latitudes from 72° to 82°N and were 168 ± 3 K throughout this region. For the slant geometry of these observations, T_{15} refers to the 0.5-mbar pressure level, about 25 km in altitude, yielding an average lapse rate over the dark regions of -2.8 K per kilometer. This is well below the adiabatic lapse rate, even ignoring a possible boundary layer, which indicates a largely stable atmosphere, although the clouds suggest some convection in the first few kilometers. The relatively high temperatures of the water ice and the atmosphere are conducive to relatively large amounts, by martian standards, of H_2O vapor in the atmosphere. High water vapor abundances were measured in simultaneous observations by the near-infrared spectrometer on the Viking orbiter (*10*).

Once a high-albedo deposit is established in the polar region, its reduced absorption of sunlight will allow it to maintain a lower temperature than unfrosted areas, and it can grow by trapping water vapor from the atmosphere at the expense of partially dehydrating warmer areas. This positive feedback behavior explains the sharp albedo and temperature contrasts of the polar region. Intrinsic to this exchange is a wind system between the frosted and dark areas, as would be expected from the 30 K temperature contrast between these two materials in the summer.

The constancy of the frost patches over 5 years and the large temperature contrasts in the polar area suggest that the water ice deposits are fairly thick, although direct measurements are not yet available (*11*). Ice thicknesses between a few centimeters, as required to extinguish the solar flux which would otherwise reach the underlying soil, and about 1 km, the presumed depth of the craters occupied, would not directly conflict with any existing observations. If the north polar ice averaged 10 m thick, it would represent 1000 times the amount amount of H_2O in the entire martian atmosphere.

Persistence of the water ice areas should be expected, as complete H_2O exchange with the saturated atmosphere on a daily basis could only move about ½ cm of ice in a martian summer. Since there is almost certainly much more H_2O in the polar caps than in the atmosphere, the polar frost areas are probably stable as long as the annual climate is not changed; it is likely that they persist over periods at least as long as half the shortest orbital precessional cycle (*12*). Because of the positive feedback discussed above, there is a potential for building very thick ice deposits. Based on the surface and atmospheric temperatures measured by the IRTM, a standard atmosphere over the dark regions would contain about 5 mg cm^{-2} of water vapor. If the outlying frost areas trap 10 percent of this water vapor on a daily basis during midsummer, they would accumulate 50 m of ice in 100,000 years.

While water ice may accumulate at the polar surface over long periods, the summertime polar environment reported here does not favor a permanent CO_2 deposit. At 5°N, 81°W, near the middle of a reservoir of solid CO_2 proposed by Murray and Malin (*3*), the measured brightness temperature was 216 K; this is 68 K higher than solid CO_2. This temperature is typical of the summer polar cap environment, and such a temperature difference for about one-fifth of the martian year represents the thermal load that any permanent CO_2 deposit would have to accommodate. It is unlikely that small areas of frozen CO_2, below the resolution of the IRTM, could exist in the polar environment observed; the temperatures would not even allow a CO_2 hydrate clathrate. The IRTM observations indicate that all of the polar condensate at this season is H_2O.

HUGH H. KIEFFER
University of California, Los Angeles 90024
STILLMAN C. CHASE, JR.
Santa Barbara Research Center, Goleta, California 93017
TERRY Z. MARTIN
University of California, Los Angeles
ELLIS D. MINER
Jet Propulsion Laboratory, California Institute of Technology, Pasadena 91103
FRANK DON PALLUCONI
Jet Propulsion Laboratory

References and Notes

1. Temperatures near 150 K, the saturation temperature of CO_2 at the mean martian surface pressure, were measured by the Mariner 7 infrared radiometer [G. Neugebauer, G. Münch, H. H. Kieffer, S. C. Chase, Jr., E. D. Miner, *Astron. J.* **76**, 719 (1971)]. The Mariner 7 infrared spectrometer gave independent spectroscopic evidence of solid CO_2 [K. C. Herr and G. C. Pimentel, *Science*, **166**, 496 (1969)].
2. A. P. Ingersoll, *J. Geophys. Res.* **79**, 3403 (1974).
3. B. C. Murray and M. C. Malin, *Science* **182**, 437 (1973).
4. G. A. Briggs, *Icarus* **23**, 167 (1974).
5. A climatic instability involving CO_2 polar caps has been proposed by C. Sagan, O. B. Toon, and P. J. Gierasch [*Science* **181**, 1045 (1973)]. Gas storage in the soil is discussed by F. P. Fanale and W. A. Cannon [*J. Geophys. Res.* **79**, 3397 (1974)].

6. The analysis of Mariner 9 radio occultation data by P. M. Woiceshyn, [*Icarus* **22**, 325 (1974)] indicates that north of 75°N the average surface pressure is 0.4 mbar greater than the martian average. A topographic map of the same region by D. Dzurisin and K. R. Blasius, [*J. Geophys. Res.* **80**, 3286 (1975)] indicates that the surface of the residual cap is on the average about 4 km higher than the unfrosted areas.
7. The Mariner 9 infrared radiometer and infrared interferometer-spectrometer did not have adequate spatial resolution to demonstrate that the frost areas of the residual north polar cap were not near 150 K. The global dust storm that occurred during the Mariner 9 mission caused considerable opacity in the atmosphere over the residual south polar cap, preventing a definite determination of the residual frost temperature.
8. The IRTM experiment is described in H. H. Kieffer, G. Neugebauer, G. Münch, S. C. Chase, Jr., E. D. Miner, *Icarus* **16**, 47 (1972); H. H. Kieffer, S. C. Chase, Jr., E. D. Miner, F. D. Palluconi, G. Münch, G. Neugebauer, T. Z. Martin, *Science* **193**, 780 (1976).
9. A buried solid CO_2 cap, which is sealed off from the atmosphere and has survived from some other climatic period, cannot be ruled out by these (and most other) observations. Although this has been suggested (*4*), a detailed theoretical treatment of its possible stability remains to be developed.
10. C. B. Farmer, D. W. Davies, D. D. La Porte, *Science* **194**, 1339 (1976).
11. On 30 September 1976, the inclination of the Viking 2 orbiter was increased to 75°. The improved viewing of the polar region by all three orbiter instruments should allow resolution of many detailed questions about these intriguing areas.
12. W. R. Ward [*J. Geophys. Res.* **79**, 3375 (1974)] has made a detailed analysis of the variation of the martian orbit and spin axis direction. The shortest period appreciably influencing the polar climate is the 175,000-year precession of the equinoxes.
13. J. Bennett has made major contributions to processing IRTM data. The assistance of P. Christensen, B. Jakosky, and A. Peterfreund, officially but totally inadequately described as data aides, is gratefully acknowledged. The imaging observations were provided by the Viking Orbiter Imaging Team, led by M. H. Carr. Financial support was provided by the NASA Viking Project Office.

18 October 1976

Soil and Surface Temperatures at the Viking Landing Sites

Abstract. *The annual temperature range for the martian surface at the Viking lander sites is computed on the basis of thermal parameters derived from observations made with the infrared thermal mappers. The Viking lander 1 (VL1) site has small annual variations in temperature, whereas the Viking lander 2 (VL2) site has large annual changes. With the Viking lander images used to estimate the rock component of the thermal emission, the daily temperature behavior of the soil alone is computed over the range of depths accessible to the lander; when the VL1 and VL2 sites were sampled, the daily temperature ranges at the top of the soil were 183 to 263 K and 183 to 268 K, respectively. The diurnal variation decreases with depth with an exponential scale of about 5 centimeters. The maximum temperature of the soil sampled from beneath rocks at the VL2 site is calculated to be 230 K. These temperature calculations should provide a reference for study of the active chemistry reported for the martian soil.*

The surface temperatures at the Viking landing sites have been measured at several times during the martian day by the infrared thermal mappers (IRTM) on the Viking orbiters (*1*). These measurements make possible a calculation of the daily temperature variation at depth in the soil and a prediction of the annual behavior of temperatures at the landing sites. This temperature information is directly applicable to a study of the peculiar chemistry reported for the martian soil and the possibility of biologic activity therein (*2*). In this work, "soil" is pragmatically defined as material too fine-grained to have its population accurately determined from Viking lander imaging, that is, less than a few centimeters (*3*). The term "surface" implies all exposed material, including blocks and possible bedrock.

The local times and viewing geometries available are governed by the spacecraft orbits. Thus far, high-resolution (8 km in diameter) observations have been possible only in the afternoon, when temperatures are not strongly dependent on thermal inertia. Observations shortly before dawn, which are the most useful for the determination of thermal inertia, have been possible only at very low resolution (about 200 km) for the Viking lander 1 (VL1) site and not at all for the Viking lander 2 (VL2) site. The temperature measurements at high resolution for both sites are reasonably uniform over the larger regions viewed at other local times; these results indicate that the thermal properties derived on the basis of low-resolution observations are probably representative of the 8-km area around each site and suggest that the landing sites are thermally uniform at a scale down to at least half this size. The landing areas were selected to be as bland as possible at the orbiter imaging resolution of 0.1 km (*4*) and to have no thermal anomalies; lander imaging reveals that at least the VL2 site is relatively monotonous at this scale (*5*).

On the basis of the initial assumption that the surface is homogeneous within the area viewed at each site, the observed temperatures were fitted by a one-dimensional thermal model, which accounts for the daily and seasonal changes of insolation and a weak interaction with the atmosphere (*6*, *7*). The physical properties affecting the model surface temperature are the albedo A, for which the values measured by the IRTM were used, the emissivity which was set equal to unity (*8*), and the thermal inertia $I = (k\rho C)^{1/2}$, where k is the thermal conductivity, ρ is the density, and C is the specific heat of the surface.

The albedos measured with near verticle viewing are 0.26 and 0.225 for the VL1 and VL2 sites, respectively; although the apparent albedo is higher at large incidence angles, probably in large part due to haze in the atmosphere, these values were adopted as constant. The resulting thermal inertias are, respectively, 9 ± 0.5 and 8 ± 1.5; the unit of I is 10^{-3} cal cm^{-2} sec^{-1} K^{-1} throughout this work. The uncertainties are not formal but rather estimates based on the limited observation geometry available and the apparent atmospheric effects present throughout much of the northern hemisphere; the large uncertainty at the VL2 site results from the lack of predawn data. As was known during Viking site certification, both of these locations have thermal inertias higher than the martian average.

The flat-lying, homogeneous model used here does not explain completely the brightness temperatures at all the local times observed (*1*); however, it should approximate the physical temperature of the surface and subsurface to within about 5 K. Based on the properties derived above, the surface temperatures at the two sites for an entire martian year were computed. Because the model parameters are derived from remote observations, these temperatures (Fig. 1) represent an area-weighted average of the soil and rocks; they represent the environmental extremes at the Viking sites. The diurnal minimum probably models well the minimum for at least the first 2 m of the atmosphere; the diurnal maximum probably models well the peak temperature of a thinner atmospheric layer (*9*).

The predicted thermal behavior of the two sites is quite different. At midday, the temperature reaches a maximum near the autumn equinox (aerocentric longitude of the sun $L_s = 180°$) rather than at midsummer and has a secondary peak near the spring equinox ($L_s = 0°$). This large semiannual behavior results from the eccentricity of the orbit of Mars, tending to offset the effect of its polar tilt in the northern hemisphere (the effects add in the southern hemisphere). The VL1 site is near the latitude which experiences the smallest annual variation of temperature.

The VL2 site, in contrast, has well-de-